CERN-PPE/90-103
18 July 1990

EUROPEAN ORGANIZATION FOR NUCLEAR RESEARCH



# Measurement of the Neutron and the Proton $F_2$ Structure Function Ratio

THE NEW MUON COLLABORATION (NMC)

*Bielefeld University[1+], Freiburg University[2+], Max-Planck Institute Heidelberg[3], Heidelberg University[4+], Indiana University[5], University of Mainz[6+], Mons University[7], Neuchâtel University[8], NIKHEF-K[9++], Oxford University[10], University of California, Santa Cruz[11], PSI[12], Torino University and INFN Torino[13], Uppsala University[14], Institute for Nuclear Studies, Warsaw[15*], Warsaw University[16**], Wuppertal University[17+]*

D. Allasia[13], P. Amaudruz[12], M. Arneodo[13], A. Arvidson[14], B. Badelek[16], G. Baum[1], J. Beaufays[9a)], I.G. Bird[3], M. Botje[12], W.J. Burger[12], C. Broggini[8], W. Brückner[3], A. Brüll[2], J. Ciborowski[9], R. Crittenden[5], R. van Dantzig[9], H. Döbbeling[3b)], J. Domingo[12], J. Drinkard[11], A. Dzierba[5], H. Engelien[2], M.I. Ferrero[13], L. Fluri[8], P. Grafstrom[14c)], D. Greiner[2], P. Gretillat[8], W. Günther[2], E. Hagberg[14], D. von Harrach[3], M. van der Heijden[9], C. Heusch[11], Q. Ingram[12], A. Jacholkowska[5d)], K. Janson[14], M.de Jong[9], E.M. Kabuß[3], R. Kaiser[2], T. Ketel[9], F. Klein[6], B. Korzen[17], U. Krüner[17], S. Kullander[14], U. Landgraf[2], F. Lettenström[14], T. Lindqvist[14], G.K. Mallot[6], C. Mariotti[13], G. van Middelkoop[9], Y. Mizuno[3], J. Nassalski[15], D. Nowotny[3], N. Pavel[17e)], H. Peschel[17], C. Peroni[13], B. Povh[3,4], R. Rieger[6], K. Rith[3], K. Röhrich[6], E. Rondio[16], L. Ropelewski[16], A. Sandacz[15], C. Scholz[3], R. Schumacher[12g)], U. Sennhauser[12], F. Sever[1h)], T.-A. Shibata[4], M. Siebler[1], A. Simon[3], A. Staiano[13], G. Taylor[10i)], M. Treichel[3j)], J.L. Vuilleumier[8], T. Walcher[6], K. Welch[5], R. Windmolders[7]

*(Submitted to Physics Letters)*

## ABSTRACT

The ratio of the structure function $F_2^n/F_2^p$ (x) has been measured in deep inelastic scattering of 274 GeV muons on hydrogen and deuterium targets exposed simultaneously to the beam. The results were obtained from 0.3 (0.6) million events from hydrogen (deuterium) in the range $0.004 < x < 0.8$ and $1 < Q^2 < 190$ GeV$^2$. At $x < 0.25$ both the statistical and the systematic error is below 2%. Implications for parton distributions and for the $\sigma_W/\sigma_Z$ production cross section ratio in $\bar{p}p$ collisions are discussed. When compared to other results obtained at lower energies, the data indicate a $Q^2$ dependence of the ratio.

+ Supported by Bundersministerium für Forschung and Technologie.
++ Supported in part by FOM and NWO.
* Supported in part by CPBP.01.06.
** Supported in part by CPBP.01.09.

a) Now at Trasys, Brussels, Belgium.
b) Now at PSI, Villigen, Switzerland.
c) Now at CERN, Geneva, Switzerland.
d) Now at Laboratoire de l'Accélérateur Linéaire, Université de Paris-Sud, Orsay, France.
e) Now at DESY, Hamburg, FRG.
f) Now at MPI für Neurologische Forschung, Köln, FRG.
g) Now at Carnegie Mellon University, Pittsburgh, U.S.A.
h) On leave of absence from Jozef Stefan Institut, Ljubljana, Yugoslavia, now at DPhN Saclay, Gif-sur-Yvette, France.
i) Now at University of Melbourne, Parkville, Victoria, Australia.
j) Now at Université de Neuchâtel, Neuchâtel, Switzerland.

In the parton picture the structure function ratio $F_2^n/F_2^p$ is sensitive to the ratio of the up and down quark distributions. Therefore, $F_2^n/F_2^p$ puts strong constraints on the flavour decomposition of the structure functions [1-7]. The parton distributions, especially in the low x region, are widely used to calculate hard scattering cross sections in $p\bar{p}$, pp and ep collisions. However, the large systematic errors in the previous measurements of the $F_2^n/F_2^p$ ratio lead to large uncertainties for the predictions [8].

Previous results on the ratio were obtained from the measurements with electron beams at SLAC [9,10] and with the high energy muon beam at CERN by the EMC [11] and the BCDMS [12] collaborations.

The New Muon Collaboration (CERN-NA37) has performed a measurement of deep inelastic muon scattering on hydrogen and deuterium simultaneously. From these measurements the x-dependence of the neutron to proton structure function ratio $F_2^n/F_2^p$ has been derived. The results cover the kinematic range of $x = 0.004 - 0.8$ and $Q^2 = 1 - 5$ GeV$^2$ for the lowest and 10 - 190 GeV$^2$ for the highest x value. Here $x = Q^2/2M\nu$ is the Bjorken scaling variable, M is the proton mass and $-Q^2$ and $\nu$ are virtual photon mass squared and energy respectively. Compared to previous measurements the present data extend to lower values of x and have smaller systematic errors.

The experiment was performed at the muon beam line M2 of the SPS at CERN. The average incident muon momentum was 274 GeV with a rms spread of 11 GeV and the integrated beam intensity was $2.4 \cdot 10^{12}$ muons. An upgraded version [13,14] of the EMC spectrometer [15], shown in fig. 1, was used.

In addition to the standard trigger (T1), which accepts muons at scattering angles larger than 10 mrad, a small-angle trigger (T2) which extends the acceptance down to 5 mrad was implemented. It selected target-pointing coincidences of three hodoscope planes (H1',H3',H4') composed of horizontal strips with a width of 1 cm. The central strips were excluded leading to a minimum vertical muon scattering angle of 5 mrad. Due to the small horizontal extension (50 cm for H4'), only events with small horizontal bending in the magnet were accepted. This removed events with $y = \nu/E_\mu > 0.6$ at the trigger level. Both triggers covered the small x region ($x < 0.4$), the T2 events having smaller $Q^2$ and $\nu$. Higher values of x were obtained by the T1 trigger only.

The longitudinal vertex resolution, being inversely proportional to the scattering angle, was improved by introducing a small (14 cm diameter) 8 plane proportional chamber (P0B) with 1 mm pitch and by upgrading the proportional chamber PV1 from a 4 mm to a 2 mm pitch (see fig. 1). In order to handle higher trigger rates, a beam spill buffering system was used allowing to buffer up to 1000 events during the 2 s spill. The 12 s interval between spills was used for event building and tape writing.

In the free space (50 m) behind the experiment a beam momentum calibration spectrometer, consisting of a precision dipole and proportional chambers with 1 mm pitch, was installed. It allowed a momentum determination with a 0.2% accuracy.

The target system consisted of two sets of target pairs which were alternately exposed to the beam which had horizontal and vertical dimensions of 1.3 cm and 1.0 cm rms respectively. Each target cell was made out of a 10 cm diameter, 3 m long mylar cell filled with liquid $H_2$ or $D_2$. The cell was contained in a hard paper vacuum container of 30 cm diameter. The two target pairs were identical except for the sequence of the target materials (see fig. 1). By a lateral transport mechanism either set could be moved into the beam. Frequent exchange of the two sets (typically twice an hour) minimised the effects of any time dependent detector response.

Figure 2, showing the longitudinal distribution of the reconstructed interaction vertices after kinematic cuts, demonstrates the excellent separation of the events from different targets. It can be seen that the spectrometer acceptance varies strongly with the vertex position. However, in the product of the counting rates, $(N_D/N_H)_{upstream}$ and $(N_D/N_H)_{downstream}$ both the acceptance and the flux cancel. Therefore, the cross section ratio was obtained for each $(x,Q^2)$ bin from

$$\frac{\sigma_d^{meas}}{\sigma_p^{meas}} = \kappa \sqrt{\left(\frac{N_D}{N_H}\right)_{upstream} \cdot \left(\frac{N_D}{N_H}\right)_{downstream}} \quad , \qquad (1)$$

where $\kappa$, the ratio of the molar volumes of the $D_2$ and $H_2$, was determined as 0.8664(6). The uncertainties in the acceptance and flux normalisation were the important sources of systematic errors in previous experiments [11,12].

Data were taken in three SPS periods of 17 days each during the years 1986 and 1987. This represents about half of the total accumulated statistics at 274 GeV. The description of the event reconstruction can be found in refs. [14,15]. Kinematic cuts were applied to remove events with large radiative corrections, poor kinematic resolution or background from hadronic decays. The following cuts were used:

| | | | | |
|---|---|---|---|---|
| $p_\mu'$ | > | 30 GeV | $x > 0.004$ | for T1 and T2, |
| $\theta$ | > | 10 mrad | $\nu > 10$ GeV | for T1, |
| $\theta$ | > | 5 mrad | $\nu > 15$ GeV | for T2, |

where $p_\mu'$ and $\theta$ are the scattered muon laboratory momentum and the scattering angle, respectively. These cuts imply $Q^2 > 1$ GeV$^2$ and $y < 0.89$ for $E_\mu = 274$ GeV. No cuts were applied to exclude data close to the edges at the acceptance. This is justified since the spectrometer acceptance cancels in the cross section ratio (1). The total number of events which

passed the cuts was 222,000 (447,000) from H(D), for T1 and 80,000 (172,000) from H(D) for T2.

The ratio of one-photon cross section $\sigma_d^{1\gamma} / \sigma_p^{1\gamma}$ was calculated from (1) after weighing each event with the corresponding radiative correction factor $\sigma^{1\gamma} / \sigma^{meas}$. The radiative correction factors for the H and D targets were calculated by using the method of Mo and Tsai [16]. The calculations require the absolute structure functions $F_2^p$ and $F_2^d$ as an input. Both $F_2$'s were determined from a fit to electron and muon scattering data down to the threshold for resonance production. Within our kinematic range, however, we determined $F_2^p$ from the measured ratio and the $F_2^d$ in an iterative procedure. The result of the iterations was found to be insensitive to the starting value of $F_2^d/F_2^p$. For T1 events the average radiative correction factor ranged from 0.64 (0.70) for H(D) events at x = 0.007 to more than 0.90 for x > 0.1. For T2 events the correction factor was about 0.80 at the lowest x. The resulting effective correction on the ratio was about 12% at x = 0.007 and was less than 1% for x > 0.1. The assumed 7% uncertainty in the absolute normalisation of $F_2^d$ gives rise, through the radiative corrections, to a systematic errror on the ratio of 1.3% at the smallest x and to less than 0.1% at x > 0.06. The assumed uncertainties in the suppression [9] of the quasielastic electric (20%) and magnetic (50%) form factors in deuterium contribute 1% and 1.4% respectively, to the systematic error on the ratio at the smallest x and less than 0.1% at x > 0.06.

In calculating the radiative corrections we have assumed the value of R, the ratio of the longitudinal to transverse polarised virtual photon - nucleon absorption cross section, to be the same for H and D targets. For x > 0.1, this assumption is consistent with measurements [17]. As a consequence we obtain

$$F_2^d/F_2^p = \sigma_d^{1\gamma}/\sigma_p^{1\gamma} \quad . \tag{2}$$

The $F_2^n/F_2^p$ ratio is defined as

$$F_2^n/F_2^p = F_2^d/F_2^p - 1 \tag{3}$$

without any correction for possible binding effects in the deuterium nucleus. In particular, we did not correct for the smearing effect due to Fermi motion. Current models [18] give insignificant corrections for x < 0.6.

The effects of the limited spectrometer resolution in x and $Q^2$ (smearing effects) on the ratio $F_2^n/F_2^p$ were determined by a Monte Carlo simulation of the experiment. The simulated

events were passed through the same chain of reconstruction programs as the real data. For T1 events the smearing correction factor, averaged over $Q^2$, changes from 1.002 to 0.995 for x varying between 0.007 and 0.55. For T2 events the biggest smearing correction factor is found to be 1.016 at x = 0.175. Figure 2 shows the separation of different target materials seen in the beam. The association of events to the wrong target was estimated from an extrapolation of the tails of the vertex distribution. The largest correction was 1%, at small x. The correction from a 3% HD admixture in liquid deuterium is 0.3% (2%) at small (large) x.

The ratios $F_2^n/F_2^p$ were calculated in x and $Q^2$ bins for each SPS period separately and they were found to be mutually consistent. The results from different periods and different $Q^2$ bins were merged taking their geometrical average [19].

The final results and their errors are given in table 1 separately for each trigger. The weighted arithmetic average of the results from both triggers is also shown in table 1 and fig. 3. The dominant contribution to the systematic error at small x comes from the uncertainties in the radiative corrections for deuterium, whereas at high x it is due mainly to the uncertainties in the beam (0.2%) and scattered muon (0.15%) momentum. The systematic errors due to vertex position smearing, $H_2$ and $D_2$ density and to target position dependent reconstruction efficiency (due to background hits in the chambers) contribute in total to less than 0.5%. The total systematic error has been calculated by adding individual contributions in quadrature. The systematic error is seen to range from 2% at small x to 0.4% at x = 0.1 and to 8% at high x.

In fig. 3 we also show the results from the BCDMS muon beam experiment [12] which covers a similar range in $Q^2$. Our data extend to smaller x and have significantly smaller systematic errors. They are in good agreement with the BCDMS results in the region of overlap. The present data are also consistent with the early EMC results [11] (not shown in the figure) within their large systematic errors. In this figure we also show the recently re-evaluated results from 1.6 - 20 GeV electron beam experiments at SLAC [17] which cover smaller $Q^2$ ($0.6 < Q^2 < 30$ GeV$^2$) and have small systematic errors. From the observed difference between the present and the SLAC results for x = 0.15 – 0.35 we obtain an average slope of $\Delta(F_2^n/F_2^p)/\Delta \ln Q^2 = -0.019(4)$. Leading order QCD calculations made using the formalism of Abbot et al. [20] predict slopes between 0 and – 0.01.

The present measurements extend below x = 0.03 to a region not covered by previous experiments. In this region, dominated by sea partons, $F_2^n/F_2^p$ depends also on the residual valence parton distribution and on the amount of a possible flavour symmetry breaking in the sea. At x = 0 the Quark-Parton Model predicts no contribution from valence partons to the structure functions. The sea partons of different flavours are believed to have the same coupling to the Pomeron which dominates the low x Regge behaviour of the virtual photon-nucleon cross section [21]. At our lowest x point (x = 0.007, $\langle Q^2 \rangle$ = 2.6 GeV, $\langle \nu \rangle \equiv$ 200 GeV) the structure function ratio is already consistent with one, indicating the

expected approach to symmetry between u and d partons in the sea for $x \to 0$. It is interesting to note that the real photon ($Q^2 = 0$) total cross section ratio $\sigma_n^{tot} / \sigma_p^{tot} = (\sigma_d^{tot} - \sigma_p^{tot}) / \sigma_p^{tot} =$ 0.898(15) at $\nu = 16 - 18$ GeV [22]. This significant deviation from unity was interpreted in terms of shadowing of real photons in deuterium [23]. Assuming no discontinuity between real and virtual photon cross sections the shadowing should also be present in virtual photon-deuterium interactions at $Q^2 \cong 0$ and similar $\nu$. The fact that we do not observe shadowing could be due to either not reaching low enough x or being too high in $Q^2$.

Parton distributions have been extracted [1-7] from simultaneous fits to hard scattering cross section data. The present high precision data at small x constrain such parameterisations in the region where valence and sea partons have comparable contributions. The most recent fit [7], in which our preliminary data [24] were also included, correctly describes the shape of the $F_2^n/F_2^p$ ratio in terms of parton distributions; see fig. 4.

As indicated in [7,8], precise data on $F_2^n/F_2^p$ reduce the uncertainty in predictions for the $\sigma_W/\sigma_Z$ production cross section ratio in $\bar{p}p$ collisions. In particular, at the Fermilab collider energy of $\sqrt{s} = 1800$ GeV the predictions are sensitive to the d/u parton ratio at $x \cong 0.05$, which can be well constrained only by our data. Calculations [7] at this energy, based on our preliminary results [24], predict $\sigma_W/\sigma_Z = 3.30$ for three neutrino families.

To summarise, the ratio $F_2^n/F_2^p(x)$ has been determined with high statistical and systematic accuracy down to $x = 0.007$. The results put strong constraints on the prediction of the parton distributions in a region where the contribution from both sea and valence partons is important. At the smallest x the $F_2^n/F_2^p$ ratio is close to unity; the shadowing of virtual photons in deuterium is not seen in the present kinematic range. The comparison of our results with those from SLAC in the x-range of 0.15 – 0.35 indicates a stronger $Q^2$ dependence of the ratio than that predicted by leading order perturbative QCD.

We wish to thank the technical staff of CERN and of the participating institutes for their invaluable contributions to the experiment. The contribution of Dr. J. Zmeskal in measuring the isotopic purity of the deuterium target is gratefully acknowledged.

## References


1. A.J. Buras and K.F.J. Gaemers, Nucl. Phys. **B132** (1978) 249.
2. M. Glück, E. Hoffman and E. Reya, Z. Phys. **C13** (1982) 119.
3. D.W. Duke and J.F. Owens, Phys. Rev. **D30** (1984) 49.
4. E. Eichten et al., Rev. Mod. Phys. **56** (1984) 579;
   for erratum see Rev. Mod. Phys. **58** (1986) 1065.
5. M. Glück, E. Reya and A. Vogt, Dortmund University report DO-TH 89/20.
6. M. Diemoz et al., Z. Phys. **C39** (1988) 21.
7. P.N. Harriman et al., University of Durham report DTP/90/04, RAL /90/007,
   revised April, 1990.
8. A.D. Martin, R.G. Roberts and W.J. Stirling Phys. Lett. **B189** (1987) 220;
   Phys. Lett. **B206** (1988) 327; Phys. Lett. **B207** (1988) 205.
9. S. Stein et al., Phys. Rev. **D12** (1975) 1884;
   A. Bodek et al., Phys. Rev. **D20** (1979) 1471.
10. M.D. Mestayer et al., Phys. Rev. **D27** (1983) 285
11. EMC, J.J. Aubert et al., Nucl. Phys. **B293** (1987) 740.
12. BCDMS, A.C. Benvenutti et al., Phys. Lett. **B237** (1990) 599.
13. D. Allasia et al., CERN report CERN/SPSC 85-18.
14. NMC, A. Simon, PhD Thesis (in German), University of Heidelberg (1988);
    NMC, D. Nowotny, PhD Thesis (in German), University of Heidelberg (1989);
    NMC, C. Broggini, PhD Thesis (in English), University of Neuchâtel (1989);
    NMC, C. Scholz, PhD Thesis (in German), University of Heidelberg (1989).
15. EMC, O.C. Allkofer et al., Nucl. Instr. and Meth. **179** (1981) 445;
    EMC, J.P. Albanese et al., Nucl. Instr. and Meth. **212** (1983) 111;
    EMC, J.J. Aubert et al., Nucl. Phys. **B259** (1985) 189.
16. L.W. Mo and Y.S. Tsai, Rev. Mod. Phys. **41** (1969) 205;
    T.S. Tsai, SLAC-PUB-848 (1971).
17. L.W. Whitlow, Ph.D. Thesis, Stanford University, 1990; SLAC-Report-357, 1990.
18. L.L. Frankfurt, M.I. Strikman, Phys. Lett **76B** (1978) 333;
    Nucl. Phys. **B181** (1981) 22;
    A. Bodek, J.L. Richtie, Phys. Rev. **D23** (1981) 1070; **D24** (1981) 1400.
19. A. Bodek, Nucl. Instr. and Meth. **117** (1974) 613; erratum **E150** (1978) 367.
20. L.F. Abbot et al., Phys. Rev. **D22** (1980) 582.
21. R.D. Field and R. P. Feynman, Phys. Rev. **D15** (1977) 2590.
22. CERN report, CERN-HERA 87-01, "Compilation of Cross Sections IV".
23. D.O. Caldwell et al., Phys. Rev. **D7** (1973) 362.
24. NMC, presented by J. Nassalski at the Europhysics Conference on High Energy
    Physics, Madrid, 1989.

## TABLE 1

The ratio $F_2^n/F_2^p$ averaged over $Q^2$

| | Trigger 1 | | | | Trigger 2 | | | | Both Triggers | | | |
|---|---|---|---|---|---|---|---|---|---|---|---|---|
| x | $\langle Q^2 \rangle$ $(GeV)^2$ | $F_2^n/F_2^p$ | $\sigma_{stat.}$ | $\sigma_{syst.}$ | $\langle Q^2 \rangle$ $(GeV)^2$ | $F_2^n/F_2^p$ | $\sigma_{stat.}$ | $\sigma_{syst.}$ | $\langle Q^2 \rangle$ $(GeV)^2$ | $F_2^n/F_2^p$ | $\sigma_{stat.}$ | $\sigma_{syst.}$ |
| 0.007 | 3.1 | 0.990 | 0.021 | 0.023 | 2.0 | 0.986 | 0.022 | 0.023 | 2.6 | 0.988 | 0.015 | 0.023 |
| 0.015 | 5.6 | 0.970 | 0.016 | 0.014 | 3.3 | 0.979 | 0.021 | 0.014 | 4.8 | 0.973 | 0.013 | 0.014 |
| 0.030 | 9.2 | 0.935 | 0.014 | 0.010 | 4.2 | 0.943 | 0.019 | 0.010 | 7.9 | 0.938 | 0.011 | 0.010 |
| 0.050 | 14.5 | 0.920 | 0.017 | 0.005 | 4.9 | 0.909 | 0.024 | 0.005 | 11.4 | 0.917 | 0.014 | 0.005 |
| 0.080 | 18.9 | 0.857 | 0.014 | 0.003 | 5.5 | 0.863 | 0.021 | 0.003 | 14.9 | 0.858 | 0.011 | 0.003 |
| 0.125 | 23.9 | 0.803 | 0.015 | 0.003 | 7.0 | 0.825 | 0.028 | 0.004 | 20.3 | 0.808 | 0.013 | 0.003 |
| 0.175 | 27.4 | 0.709 | 0.017 | 0.003 | 8.2 | 0.879 | 0.042 | 0.004 | 24.8 | 0.732 | 0.016 | 0.003 |
| 0.250 | 31.3 | 0.697 | 0.015 | 0.003 | 10.2 | 0.700 | 0.044 | 0.007 | 29.0 | 0.698 | 0.014 | 0.003 |
| 0.350 | 35.5 | 0.572 | 0.019 | 0.004 | 13.6 | 0.723 | 0.096 | 0.012 | 34.6 | 0.578 | 0.019 | 0.004 |
| 0.450 | 36.3 | 0.562 | 0.027 | 0.006 | | | | | 36.3 | 0.562 | 0.027 | 0.006 |
| 0.550 | 36.4 | 0.529 | 0.037 | 0.011 | | | | | 36.4 | 0.529 | 0.037 | 0.011 |
| 0.700 | 33.5 | 0.292 | 0.036 | 0.024 | | | | | 33.5 | 0.292 | 0.036 | 0.024 |

## Figure Captions

Fig. 1 The New Muon Collaboration spectrometer. The beam momentum calibration spectrometer located downstream of the apparatus is not shown.

Fig. 2 The distribution of the reconstructed vertex position along the beam for the analysed T1 events. Full symbols are for the runs with $(D_2)_{upstream}$- $(H_2)_{downstream}$ target set while open symbols are for the complementary target set. The drawing on the top shows positions of the targets and detectors seen in the distribution.

Fig. 3 The ratio $F_2^n/F_2^p$ (x) from this experiment compared to previous results from SLAC [17] and BCDMS [12]. The contours show the size of the systematic errors.

Fig. 4 The ratio $F_2^n/F_2^p$ (x) compared to the parameterisation (HMRSB) of ref. [7].

# NMC SPECTROMETER (TOP VIEW)

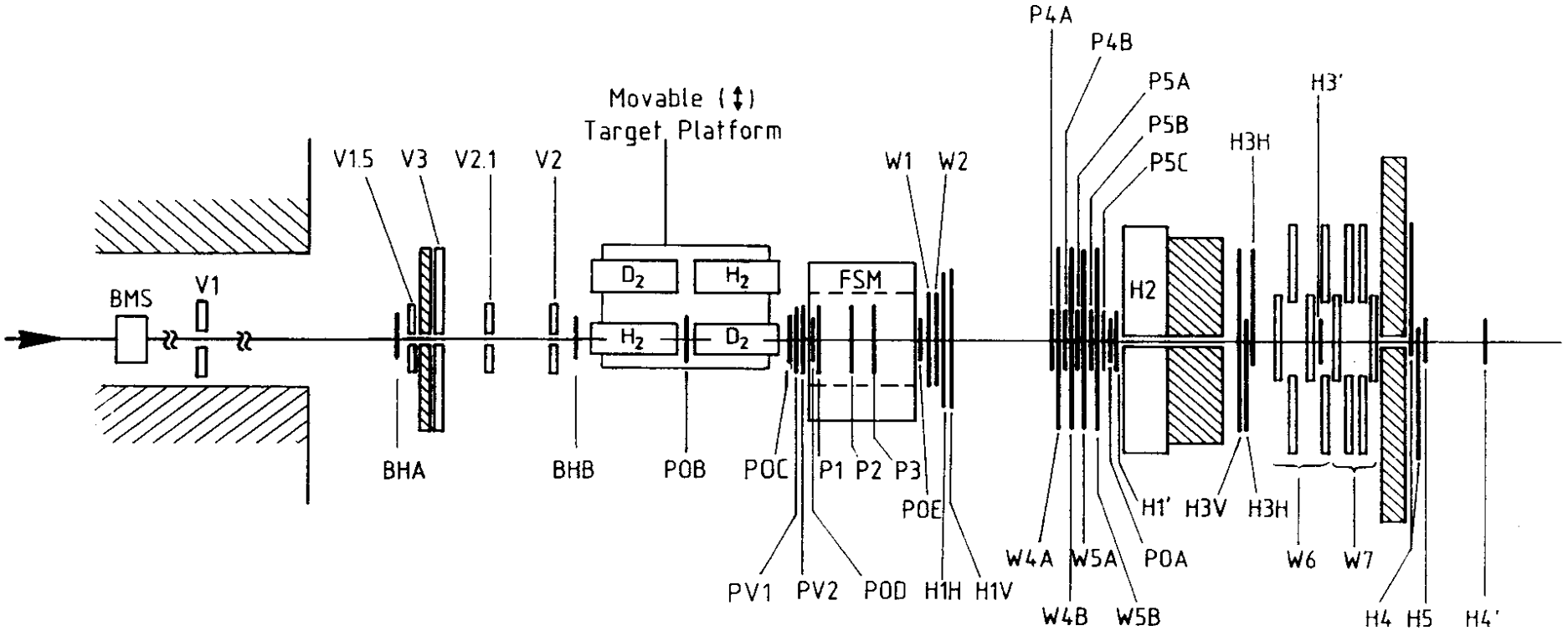


| | |
|---|---|
| BMS | Beam momentum station |
| V1,V15,V3,V2.1,V2 | Veto counters |
| BHA,BHB | Beam hodoscopes |
| POA-E,PV1-2,P1-3,P4A-5C | Proportional chambers |
| FSM | Forward spectrometer magnet |
| W1-2,W4A-5B,W6-7 | Drift chambers |
| H1H,H1V,H3V,H3H,H4,H5 | Large angle trigger hodoscopes |
| H1',H3',H4' | Small angle trigger hodoscopes |
| H2 | Hadron calorimeter |
| | Iron absorbers |

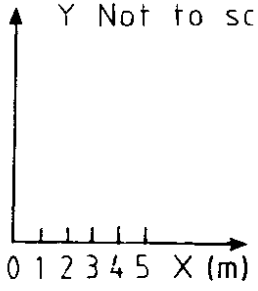


FIG. 1

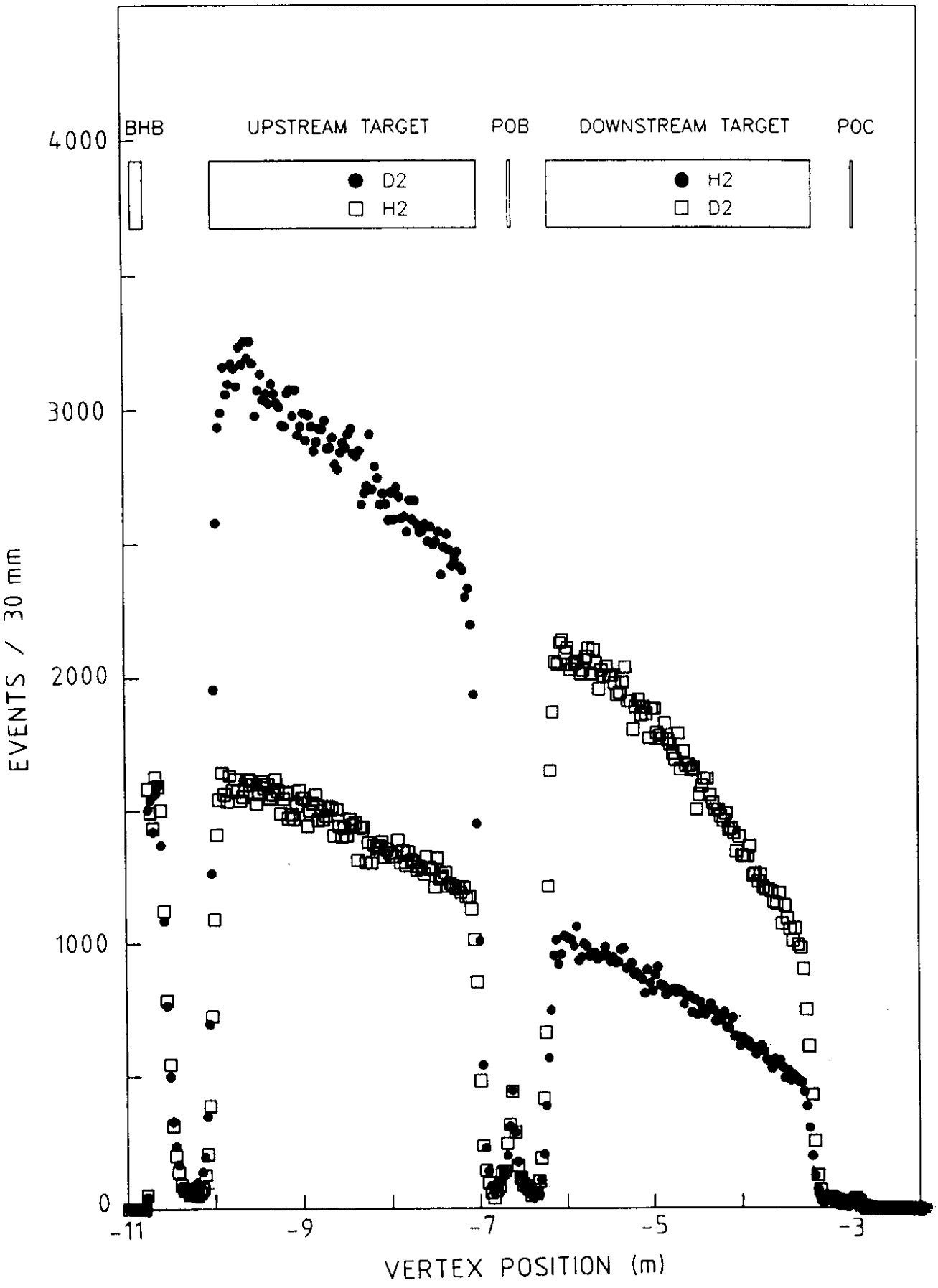
BHB
UPSTREAM TARGET
POB
DOWNSTREAM TARGET
POC
D2
H2
H2
D2
4000
3000
2000
1000
0
EVENTS / 30 mm
-11
-9
-7
-5
-3
VERTEX POSITION (m)

FIG. 2

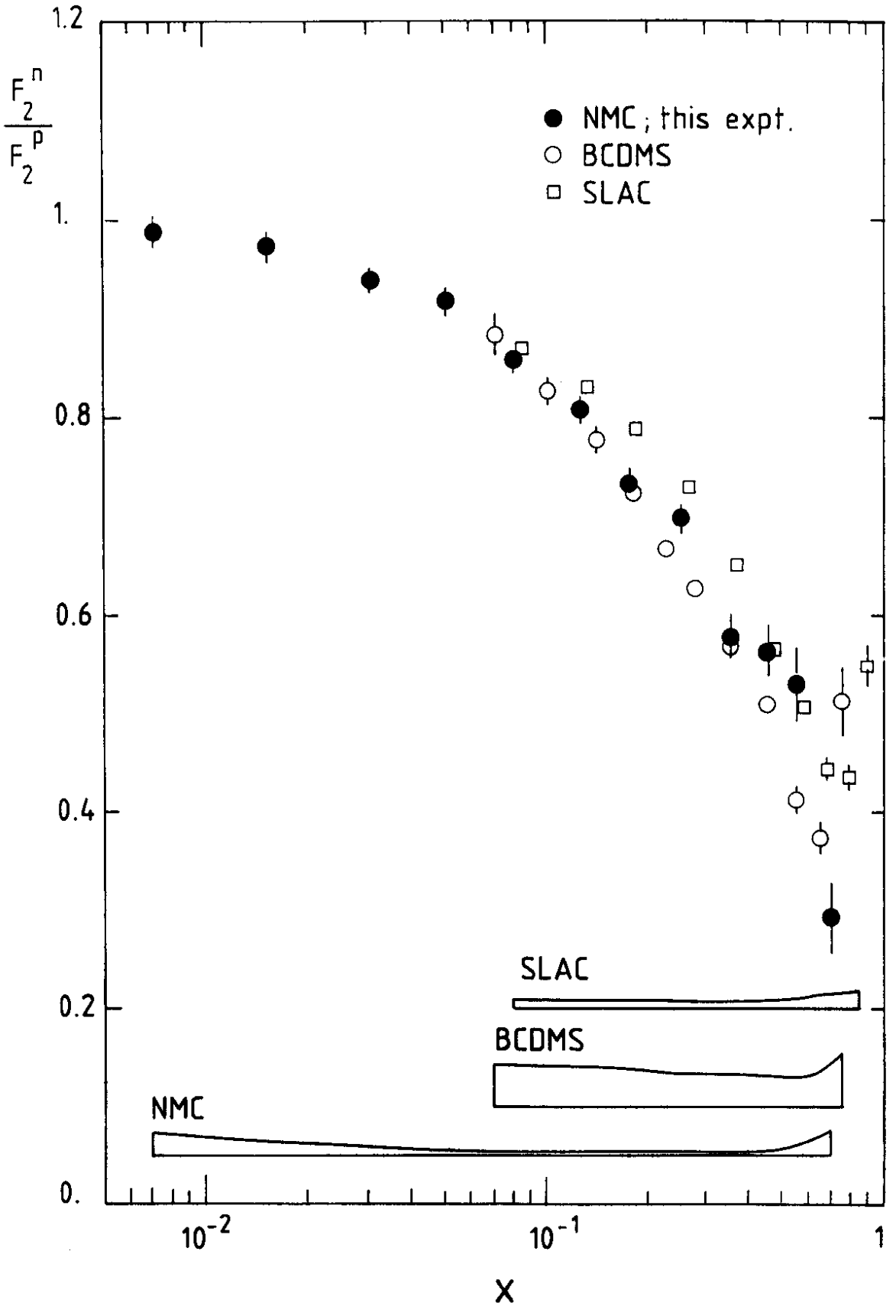
1.2
1.
0.8
0.6
0.4
0.2
0.
$\frac{F_2^n}{F_2^p}$
NMC ; this expt.
BCDMS
SLAC
SLAC
BCDMS
NMC
$10^{-2}$
$10^{-1}$
1
X

FIG. 3

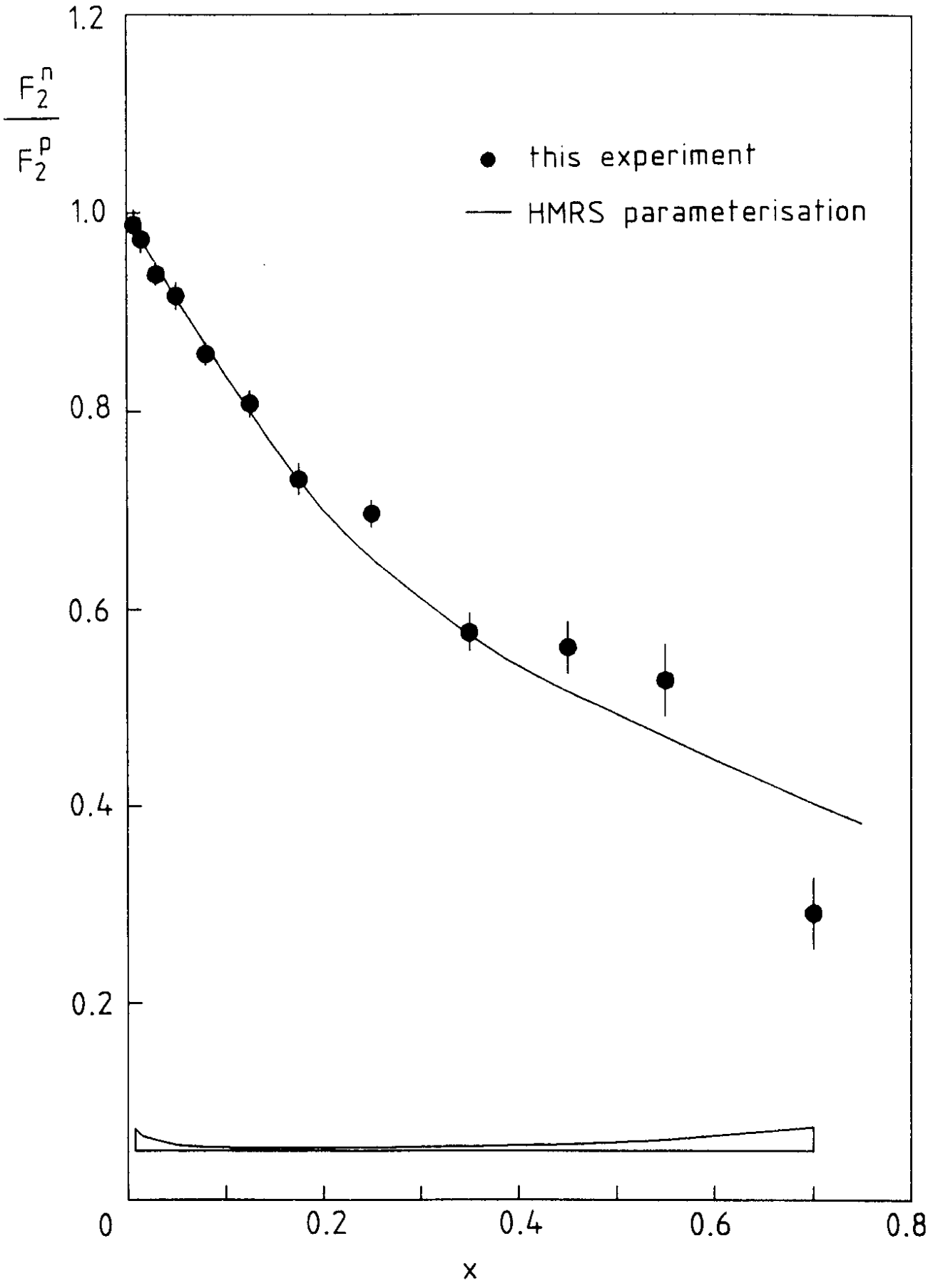


FIG. 4

Imprimé au CERN. Prix : 0.40 Fr.